

3  
4 **Running title:** Expression of Tmem41b and MMP13 in osteosarcomas

5  
6 **Expression of Tmem41b and MMP13 associated with poor outcome in osteosarcomas**

7  
8 Guo-Hua Li<sup>1,2</sup>, Xiao Liu<sup>3</sup>, Lin-Jie Feng<sup>1</sup>, Liu Zhang<sup>1,\*</sup>

9  
10 <sup>1</sup>Department of Surgical Medicine, Hebei Medical University, Shijiazhuang, Hebei, China;  
11 <sup>2</sup>Department of Orthopedics, No.2 Hospital of Tangshan, Tangshan, Hebei, China; <sup>3</sup>Department of  
12 Infection Control, The Fourth Hospital of Hebei Medical University, Shijiazhuang, Hebei, China

13  
14 \*Correspondence [zhliu130@sohu.com](mailto:zhliu130@sohu.com)

15  
16 **Received December 9, 2020 / Accepted February 19, 2021**

17  
18 Osteosarcoma (OS) is a malignant bone sarcoma characterized by a propensity for metastatic spread.  
19 Tmem41b is a multi-spanning membrane protein that acts as a novel autophagy-related (ATG) gene;  
20 however, its effect on the malignant phenotypes of tumor cells and the corresponding molecular  
21 details remains unknown. In the current study, RNA-sequencing, quantitative PCR (qPCR), and  
22 immunohistochemical analysis were conducted to prove Tmem41b upregulation in 103 OS tissue  
23 specimens and three OS cell lines (U-2OS, U87, and MG63). It was strongly correlated with tumor  
24 size ( $P < 0.01$ ), metastases ( $P < 0.05$ ), and recurrence ( $P < 0.05$ ) as well as poor survival time in OS  
25 patients. Subsequently, gene set enrichment analysis (GSEA) of U-2OS cells with Tmem41b  
26 knockdown links cell receptor activation, proliferation, and invasion according to RNA-sequence,  
27 and PCNA, Cyclin D1, Cyclin E1, and MMP13 expression levels were decreased by western  
28 blotting assay. Furthermore, the suppressive effect of Tmem41b knockdown on cell proliferation  
29 and invasion was demonstrated in vitro and in vivo. Additionally, Tmem41b silencing could  
30 significantly inhibit the AKT and p38 signaling pathways. Last, MMP13 upregulation was  
31 positively correlated with Tmem41b expression and poor survival time in OS patients via analysis  
32 of immunohistochemical detection and bioinformatics. All together, these findings demonstrate the  
33 role of Tmem41b and MMP13 as a novel prognostic marker and an attractive therapeutic target for  
34 OS.

35  
36 **Key words:** osteosarcoma; Tmem41b; MMP13; proliferation; invasion

37  
38  
39 Osteosarcoma (OS) represents a widespread malignant primary bone sarcoma in humans [1]. It  
40 accounts for approximately 20% of all bone tumors and 5% of pediatric tumors [2] and is  
41 characterized by high tumor cell proliferation, mortality, and metastatic rates [3]. This condition is  
42 most commonly seen in patients aged  $< 25$  year (60%) and in 5% of pediatric tumors [4]. Most  
43 sub-types of OS are characterized by the production of osteoid bone by malignant cells with a

44 propensity for metastatic spread, particularly to the lungs [5]. OS patients have a poor prognosis  
45 with a 5-year survival rate of < 20% using the traditional methods of treatment, including  
46 chemotherapy, wide tumor resection, and amputation [6]. Thus, the pathogenesis of the growth and  
47 invasion of OS should be deeply understood to prevent, treat, and improve patient survival.

48 The development and tumorigenesis of OS is relative to alteration of numerous molecular, including  
49 gene sequence abnormalities, chromosomal rearrangements, epigenetic change and dysregulation of  
50 signaling pathways [4]. The inhibition of rubidium (Rb) and the p53 tumor suppression signal  
51 pathways [7] and the hyperactivation of receptor tyrosine kinases (RTKs) [8] and EGFR pathways  
52 [9], ERK/MAPK pathway [10], and PI3K/AKT pathway [11], which participated in tumor cell  
53 proliferation, migration, and invasion, have been found in OS, whereas the exact mechanisms  
54 involved in these processes remain unclear.

55 Transmembrane protein 41 (Tmem41b) is an evolutionarily conserved transmembrane protein first  
56 identified as an essential requirement for the development of normal neurotransmission in mammals  
57 [12]. Recently, numerous studies showed that Tmem41b is a novel regulator of autophagy and lipid  
58 mobilization and is involved in the formation of autophagosomes [13-16]. Furthermore, some  
59 studies have reported that autophagy signaling can affect tumor cell proliferation and invasion in  
60 pancreatic cancer [17], renal carcinoma [18], and OS [10]. Meanwhile, AKT and MAPK signaling  
61 pathway also induce autophagy to promote proliferation and increase anti-cancer drug resistance  
62 [19, 20]. Notably, Tmem41b is one of the most significantly mutated genes in the lung  
63 neuroendocrine tumor spectrum, which affects cellular metabolism, immune regulation, cell cycle,  
64 apoptosis, and cell death [21]. Additionally, abnormal Tmem41b expression has been observed in  
65 OS, according to the Gene Expression Omnibus (GEO) database [22], indicating that Tmem41b  
66 may be involved in tumorigenesis and the development of OS. Yet, surprisingly, to the best of our  
67 knowledge, studies on the role of Tmem41b in OS are still lacking.

68 Thus, this research intended to identify the relationship between Tmem41b expression and the  
69 clinicopathological features of OS, as well as to investigate the roles of Tmem41b in OS cell  
70 proliferation and invasion.

71

## 72 **Patients and Methods**

73 **OS tissue specimens.** Tumor tissue specimens and the corresponding para-cancer tissues (control)

74 were obtained from 103 patients diagnosed with OS from orthopedic operation at the Orthopedics  
75 department of the Tangshan Second Hospital between January 2014 and December 2019. The  
76 samples were divided into two parts: one was snap-frozen in liquid nitrogen, and the other was  
77 paraffin-embedded. The patients with OS were staged according to the Enneking staging system  
78 [23]. All subjects provided written informed consent. The study protocol was approved the Ethics  
79 Committee of the Tangshan Second Hospital.

80 **RNA-sequence analysis.** Total RNA was extracted and quantified, as well as the mRNA profiles  
81 were detected in the three tumor tissue samples obtained from patients with OS and the  
82 corresponding para-cancer tissues (control) as well as from U-2OS cells transfected with  
83 si-Tmem41b or si-NC by Illumina HiSeq 2000. Libraries were sequenced using  $1 \times 58$  bp  
84 single-end reads, with two indexed samples per lane, yielding about 32.5 million reads per sample.  
85 After alignment of the sequencing reads to the human genome, counts for each gene were computed  
86 for each sample by use of the HTSeq software (version v0.5.3p3).

87 Differentially expressed mRNAs were identified using the paired *t*-test. A gene set enrichment  
88 analysis (GSEA) was conducted for further analysis of the biological pathways involved in the  
89 pathogenesis of OS through the Tmem41b pathway according to RNA-sequencing data.

90 **Immunohistochemistry (IHC).** Tumor tissues were fixed in 10% formalin followed by paraffin  
91 embedding and sectioning at  $4 \mu\text{m}$ , which were dewaxed, rehydrated and subjected to  
92 microwave-induced antigen retrieval. Subsequent to blocking endogenous peroxidase activity, the  
93 sections were incubated with the primary antibodies against Tmem41b (1:100) overnight at  $4^\circ\text{C}$ .  
94 Immunohistochemistry was performed using SP method immunohistochemical kit (PH1699,  
95 Phygene, Life science). The slides were analyzed and images were captured using an Olympus  
96 BX60 microscope (Olympus Corporation, Tokyo, Japan). Sections that are known to stain positively  
97 were incubated in each batch and negative controls were also established by replacing the primary  
98 antibody with pre-immune serum.

99 The results of IHC staining were evaluated independently by two trained pathologists who were  
100 blind to the clinical data. The specimens were graded into three groups according to the extent of  
101 positivity as follows: negative, no positive stain; low,  $< 25\%$  of the tumor cells showed positive  
102 stain; and high,  $> 25\%$  of tumor cells showed positive stain. The slides were re-examined by the  
103 pathologists together, and an agreement was reached for the final evaluation.

104 **Bioinformatics analysis.** The overall survival analysis of OS patients was conducted from the  
105 GEPIA dataset (Gene Expression Profiling Interactive Analysis) (<http://gepia.cancer-pku.cn>).

106 **Cell culture.** The human osteosarcoma cell lines (U-2OS, U87, and MG63) and human osteoblast  
107 cell line Hob were obtained from American Type Cell Culture (ATCC). All three cell lines were  
108 cultured in a Dulbecco's modified eagle medium (DMEM) supplemented with 10% fetal bovine  
109 serum and 100 U/ml penicillin/streptomycin (Gibco, Carlsbad, CA, USA) in a humidified  
110 atmosphere with 5% CO<sub>2</sub> at 37 °C.

111 **Cell transfection.** Specific siRNA against Tmem41b and the indicated constructs were purchased  
112 from GenePharma (Suzhou, China). The siRNA sequences of the Tmem41b duplex were as follows:  
113 5'-CACATCTTCAGCACCGCTCGTCAGATGTGGAGAAACGTCAAGAGCTTTTTTG-3' and  
114 5'-GTCCAAAAAAGCTTTTTGCAGCACATCCGTCTCAATGTGGCTGAAGAACAGC-3'.

115 The transfection was conducted through mixing of lipo2000 (Invitrogen, Carlsbad, CA, USA) with  
116 the siRNA, and the mixture was added to the cells and incubated for 6 h. DMEM (10% FBS) was  
117 then used for substitution and 24 h incubation, following subsequent cell treatment and collection.  
118 qPCR and western blotting were used to validate the transfection efficiency of Tmem41b siRNA 24  
119 h after transfection.

120 **Lentivirus infection.** The pLVX-AcGFP-Tmem41b lentiviral vector and the corresponding  
121 pLVX-AcGFP-C1 lentiviral vector (NC) were constructed by GenePharma (Suzhou, China),  
122 respectively. Lentivirus infection for 48 h in U-2OS cells inhibits Tmem41b expression. GFP  
123 fluorescence expression confirms lentiviral infection efficiency. QPCR detection was performed to  
124 verify the suppression of Tmem41b expression.

125 **Cell proliferation assay.** CCK-8 assay was used to detect the proliferation effects of Tmem41b on  
126 U-2OS cells (Dojindo, Rockville, MD, USA) assay. Briefly, transfected U-2OS cells and control  
127 were plated in 96-well plates ( $1 \times 10^4$  cells per well). CCK-8 solution (100  $\mu$ l/well) was added at  
128 different time point (0, 24, 48, and 72 h), and then were cultured for 1 h. Absorbance (450 nm) was  
129 measured using the Multiskan EX plate reader (Thermo Fisher Scientific Inc., Waltham, MA, USA)  
130 for quantification of the reaction product.

131 **Cell invasion assay.** Analysis of cell invasion by Transwell assay was referenced by modified  
132 Boyden chamber (BD, San Diego, CA, USA). Transfected U-2OS cells and control ( $1 \times 10^5$ ) were  
133 plated in the top chamber of the insert pre-coated with Matrigel, the number of transmigrated cells

134 through the membrane was counted by hematoxylin-eosin staining (HE) staining and light  
135 microscopic examination.

136 **Quantitative real time PCR.** The extraction of total RNA and qRT-PCR assay were conducted as  
137 described previously [22]. The primers sequences used were as follows: Tmem41b,  
138 5' -ATGGCGAAAGGCAGAGTCG-3' and 5' -ACCCAGGATTTTTCCTTCTGG-3' ; MMP13,  
139 5' -CTTGACCACTCCAAGGACCC-3' and 5' -CAGGCGCCAGAAGAATCTGT-3' ; Sp2,  
140 5' -GTCGTAATGAGCGATCCACAG-3' and 5' -AAGCAGGGCTAAGGGAGATG-3' ; Klk11,  
141 5' -AACCCAGCCTACCTGCTGT-3' and 5' -CCCCAGGTTCTAGGCTCT-3' ; Fkbp11,  
142 5' -AGAGACGTTGCTCTTCCGTG-3' and 5' -ATCTACCAAGCTTCCCCTG-3' ; Slc22a17,  
143 5' -TACCCCGCAGACAGATTTGG-3' and 5' -CGGTGATCATTCGGCATCAG-3' ; Nr4a2,  
144 5' -GGTCCCTTTTGCCTGTCCA-3' and 5' - GCCTGTCCAATCTCCTCCTTAG-3' ; Dtx2,  
145 5' -GAGTTTCACTCTGGCTGCCT-3' and 5' - GCTGAGGAGGACAAGAGGAC-3' ;  
146 Hist1h2af, 5' - GCACCGTCTGCTTTACAAGG-3' and 5' - GCTCCTCATCGTTGCGAATG-3' ;  
147 Crtp, 5' -GCTCAGTGGTTGCTGTTTGG-3' and 5' - GCAGTGGCCACAAGGAGTAT-3' ;  
148 GAPDH: 5' -CACCCACTCCTCCACCTTTG-3' and 5' -CCACCACCCTGTTGCTGTAG-3' .

149 **Western blotting assay.** Total proteins were extracted from treated U-2OS cells and control as well  
150 as tumor tissues via RIPA lysis buffer (Beyotime, Beijing, China) with protease inhibitors, and the  
151 protein concentrations were measured by BCA kit. SDS-PAGE (10%) was used to separate proteins,  
152 which were transfected to PVDF membrane. After blocking in 5% BSA, it was subjected to  
153 incubation using primary antibodies against PCNA (1:1000, 10205-2-AP, Proteintech), Cyclin D1  
154 (1:1000, 26939-1-AP, Proteintech), Cyclin E1 (1:1000, 11554-1-AP, Proteintech), MMP13 (1:1000,  
155 18165-1-AP, olProteintech), Tmem41b (1:1000, PA553257, Thermo), LC3B (1:2000, #2775, Cell  
156 Signaling), p62 (1:2000, #5114, Cell Signaling), AKT (1:1000, 60203-2-Ig, Proteintech), p-AKT  
157 (1:1000, 66444-1-Ig, Proteintech), ERK (1:1000, 11257-1-AP, Proteintech), p-ERK (1:1000,  
158 28733-1-AP, Proteintech), p38 (1:1000, 14064-1-AP, Proteintech), p-p38 (1:500, bs-0636R-2,  
159 Bioss), and anti- $\beta$ -actin (1:5000, 20536-1-AP, Proteintech) overnight at 4 °C. After washed in TBST,  
160 membranes were then incubated with the HRP-conjugated secondary antibody (1:8000, Rockland)  
161 for 1 h at room temperature. All images were obtained with the ECL detection system (Cell  
162 Biosciences, Santa Clara, CA.).

163 **In vivo experiments.** In this study, 24 male nude mice (6-week-old) were randomly grouped into

164 two groups (12 mice/group), and U-2OS cells ( $2 \times 10^8$ ) infected with pLV-Vector or pLV-Tmem41b  
165 for 48 h and then was injected subcutaneously into the right flank of mice to establish the  
166 osteosarcoma xenograft model. Four weeks after injection, the isolated tumor volume was measured  
167 and then was weighed. The Experimental Animal Care Commission of Hebei Medical University  
168 approved all the experiments.

169 **Statistical analysis.** All data are mean determinations of three independent experiments. The  
170 statistical analysis was conducted using GraphPad Prism 8.0 software (San Diego, CA, USA)  
171 including ANOVA post-hoc tests (Bonferroni), Chi-square test and Student's t-test for cell  
172 proliferation, cell number, band density, gene expression. Overall survival regarding OS patients  
173 was evaluated using the Kaplan-Meier survival curve and the log-rank non-parametric test. A  
174 two-sided p-value  $< 0.05$  was considered statistic significant for all tests.

175

## 176 **Results**

177 **Up-regulation of Tmem41b expression is associated with poor survival in human**  
178 **osteosarcomas tissues.** RNA-sequence was conducted to detect the mRNA expression profiles in  
179 the three tumor tissue samples from the patients with OS and the corresponding para-cancer tissues  
180 (control). As shown in Figure 1A, the top 50 mRNAs with significant differential expression  
181 patterns are listed according to a cut-off value of 2.0-fold. Furthermore, RT-qPCR validation  
182 showed that Tmem41b (15.3-fold) and MMP13 (18.7-fold) were most up-regulated in the human  
183 OS tissues (Figure 1B). In the IHC analysis, high levels of Tmem41b expression were observed in  
184 74 OS tissues, whereas 21 samples presented with low expression levels; negative expression was  
185 observed in eight tissue samples (Figure 1C).

186 Table 1 lists the clinical pathological details of the 103 OS patients, whom were grouped through  
187 the mean level of Tmem41b expression. Correlation analysis indicated that its expression was  
188 positively correlated with tumor size, metastases as well as recurrence. Furthermore, the overall  
189 survival time in OS patients with low Tmem41b expression was significantly higher than that in  
190 patients with high Tmem41b expression ( $p=0.038$ , Figure 1D). Similarly, the overall survival time  
191 of 262 OS patients from the GEPIA dataset verified that patients with high Tmem41b expression  
192 have low survival rates ( $p=0.002$ , Figure 1E). The above results showed that Tmem41b may be a  
193 promising prognostic factor in OS patients.

194 **Tmem41b knockdown affects the proliferation and invasion of OS cells.** To further validate  
195 Tmem41b up-regulation is associated with OS, we examined Tmem41b expression in three cell  
196 lines (U-2OS, U87, and MG63) and in human osteoblast cell line Hob (control). The Western  
197 blotting assay showed that Tmem41b expression was significantly higher in OS cells than in control,  
198 and the highest expression was observed in the U-2OS cells (Figure 2A). Tmem41b expression was  
199 knocked down by transfecting the OS cells with Tmem41b-specific siRNA (si-Tmem41b) or  
200 nonspecific siRNA (si-NC). The results of the qPCR and Western blot demonstrated the marked  
201 attenuation of Tmem41b expression in the si-Tmem41b-transfected cells compared with the  
202 si-NC-transfected cells (Figures 2B, 2C). Meanwhile, expression of cell autophagy-associated  
203 protein LC3II and p62 was also significantly down-regulation (Figure 2C). Furthermore, GSEA  
204 analysis indicated knockdown of Tmem41b in U-2OS cells mainly affected the genes related to  
205 receptor activity, cyclin-dependent protein, and metastasis process (Figure 2D). Consequently, the  
206 down-regulation of the proliferation- and invasion-associated proteins was verified (Figure 2E).  
207 Collectively, the above results suggest that Tmem41b expression promotes OS cell proliferation and  
208 invasion.

209 **Tmem41b knockdown suppresses cell proliferation and invasion.** Subsequently, it was found  
210 that the si-Tmem41b-transfected U-2OS cells exhibited decreased proliferation (Figure 3A) and  
211 invasion (Figure 3B) by CCK8 and Transwell assays, respectively. Additionally, these findings were  
212 further confirmed in the xenograft nude mice model. As shown in Figures 3C-3F, xenograft nude  
213 mice induced by a subcutaneous injection of U-2OS cell infected with pLV-Tmem41b or  
214 pLV-Vector after 4 weeks demonstrated a significant decrease in tumor volume (Figures 3D, 3E)  
215 and weight (Figure 3F) in pLV-Tmem41b group compared with that from pLV-Vector, and  
216 accompanied by a decreased Tmem41b expression (Figure 3C). These results indicated the effects  
217 of Tmem41b on the proliferation and invasion of OS cells.

218 **Tmem41b knockdown suppressed the AKT and p38 signaling pathways and MMP13  
219 expression.** Further experiments using Tmem41b-knockdown U-2OS cell lines were conducted to  
220 confirm whether Tmem41b involved in the proliferation and invasion of OS cells associated with  
221 the activation of the ERK, AKT, and p38 signaling pathways. As shown in Figure 4A, the  
222 knockdown of Tmem41b markedly decreased phosphorylated AKT (p-AKT) and p38 levels in the  
223 U-2OS cells, indicating that Tmem41b-induced cyclin D/E and MMP13 expression positively

224 regulates p-AKT and p-p38 signaling. Furthermore, IHC analysis proved that MMP13 expression  
225 was positive correlated with Tmem41b expression in the OS tissues (Figure 4B). Simultaneously,  
226 the overall survival time of patients with low MMP13 expression was notably higher than that of  
227 patients with high MMP13 expression levels ( $p < 0.01$ ;  $n=103$ ; Figure 4C). Similarly, the overall  
228 survival time of 262 OS patients from the GEPIA dataset indicated that patients with high MMP13  
229 expression had a shorter overall survival time (Figure 4D). Conclusively, Tmem41b knockdown  
230 attenuated the proliferation and invasion of OS cells through the inhibition of cyclin D/E and  
231 MMP13 expression via the AKT and p38 signaling pathways.

232

### 233 **Discussion**

234 In this study, we present the strong evidence of the important role of Tmem41b in the proliferation  
235 and invasion of OS cells. Tmem41b expression in OS patients was higher than that in patients with  
236 bone cysts. OS patients with high expression levels of Tmem41b and MMP13 had significantly  
237 shorter survival periods. Furthermore, Tmem41b down-regulation inhibited OS cell proliferation  
238 and invasion by suppressing the AKT and p38 signaling pathway and the expression of cyclin  
239 D1/E1 and MMP13. The bioinformatics analysis further validated that Tmem41b expression may be  
240 a diagnostic biomarker for OS.

241 Tmem41b is an integral endoplasmic reticulum membrane protein and functions as a novel  
242 regulator of autophagosome biogenesis and lipid droplet dynamics [13-15]. Recently, two  
243 documents have reported that Tmem41b was the most significantly mutated gene in neuroendocrine  
244 prostate cancer [24] and pulmonary carcinoid tumors; additionally, it was found to affect the  
245 cancer-relevant pathways and biological processes, including the MAPK/ERK pathway [19]. The  
246 proliferation of NSCLC cells can be effectively inhibited by targeting the autophagy-related 2B  
247 (ATG2B) expression [25]. Hence, we presumed that the knockdown of the autophagy-related  
248 Tmem41b expression could have a similar effect on cell proliferation and invasion. Expectedly, the  
249 results of the correlation analysis in this study showed that Tmem41b up-regulation was strongly  
250 related to tumor size ( $p < 0.01$ ), metastases ( $p < 0.05$ ), and recurrence ( $p < 0.05$ ).

251 Furthermore, Tmem41b expression levels in both human OS tissues and cultured OS cells were  
252 significantly higher than those in the corresponding controls; the highest levels were observed in  
253 U-2OS cell lines. Therefore, U-2OS cells were used in the subsequent experiments using RNA

254 knockdown to investigate the roles of Tmem41b in OS. The results of the GSEA analysis of  
255 RNA-seq detection indicated that the related gene enrichments for receptor activity,  
256 cyclin-dependent protein, and metastasis process were decreased in si-Tmem41b group, which  
257 guided us to further explore whether Tmem41b down-regulation involved in the inactivation of the  
258 biological pathway-associated proteins. As expected, Tmem41b knockdown tremendously reduced  
259 the levels of the cell cycle-associated proteins (PCNA, cyclin D1, and cyclin E) and the  
260 invasion-associated protein MMP13 [26], suggesting that Tmem41b may be an essential upstream  
261 molecule in the proliferation and invasion-associated signal pathways involved in the tumorigenesis  
262 and progression of OS.

263 Numerous studies have reported that the regulation of the ERK [27], AKT [28], and p38 [29]  
264 signaling pathways can significantly attenuate the growth and invasion of OS. Consistently, the  
265 down-regulation of Tmem41b decreased cyclin D/E and MMP13 expression levels in the U-2OS  
266 cells and suppressed cell growth and invasion via the inhibition of the AKT and p38 signaling  
267 pathways in the present study. Additionally, the inhibition of Tmem41b expression suppressed  
268 tumor growth in vivo, demonstrating that it will become a potential therapeutic target for the OS.

269 To conclude, our findings demonstrated that Tmem41b is of great significance in the tumorigenesis,  
270 progression, and prognosis of OS in humans. Tmem41b expression is significantly enhanced in  
271 human OS tissues. The dismal prognosis of OS patients can be predicted by the high expression  
272 levels of Tmem41b. Additionally, the proliferation and invasion of U-2OS cells were inhibited  
273 following the down-regulation of Tmem41b expression in vitro and in vivo. Thus, Tmem41b may  
274 prove valuable as an independent potential prognostic biomarker for patients suffering from OS.

275

276

## 277 **References**

- 278 [1] AL-KHAN AA, NIMMO JS, TAYEBI M, RYAN SD, SIMCOCK JO et al. Parathyroid  
279 hormone receptor 1 (PTHr1) is a prognostic indicator in canine osteosarcoma. *Sci Rep*  
280 2020; 10: 1564. <https://doi.org/10.1038/s41598-020-58524-3>
- 281 [2] LU Q, LV G, KIM A, HA JM, KIM S. Expression and clinical significance of extracellular  
282 matrix metalloproteinase inducer, EMMPRIN/CD147, in human osteosarcoma. *Oncol Lett*  
283 2013; 5: 201-207. <https://doi.org/10.3892/ol.2012.981>
- 284 [3] BYRGAZOV K, ANDERSON C, SALZER B, BOZSAKY E, LARSSON R et al. Targeting  
285 aggressive osteosarcoma with a peptidase-enhanced cytotoxic melphalan flufenamide. *Ther*  
286 *Adv Med Oncol* 2020; 12: 1758835920937891. <https://doi.org/10.1177/1758835920937891>

- 287 [4] MOORE DD, LUU HH. Osteosarcoma. *Cancer Treat Res* 2014; 162: 65-92.  
288 [https://doi.org/10.1007/978-3-319-07323-1\\_4](https://doi.org/10.1007/978-3-319-07323-1_4)
- 289 [5] CHEN T, ZHAO L. Patrolling monocytes inhibit osteosarcoma metastasis to the lung. *Aging*  
290 (Albany NY) 2020; 12: 23004-23016. <https://doi.org/10.18632/aging.104041>
- 291 [6] CAO M, ZHANG J, XU H, LIN Z, CHANG H et al. Identification and development of a  
292 novel 4-Gene immune-related signature to predict osteosarcoma prognosis. *Front Mol Biosci*  
293 2020; 7: 608368. <https://doi.org/10.3389/fmolb.2020.608368>
- 294 [7] HSU JH, HUBBELL-ENGLER B, ADELMANT G, HUANG J, JOYCE CE et al.  
295 PRMT1-mediated translation regulation is a crucial vulnerability of cancer. *Cancer Res*  
296 2017; 77: 4613-4625. <https://doi.org/10.1158/0008-5472.CAN-17-0216>
- 297 [8] CHIABOTTO G, GRIGNANI G, TODOROVIC M, MARTIN V, CENTOMO VL et al.  
298 Pazopanib and Trametinib as a Synergistic Strategy against Osteosarcoma: Preclinical  
299 Activity and Molecular Insights. *Cancers (Basel)* 2020; 12: 1519.  
300 <https://doi.org/10.3390/cancers12061519>
- 301 [9] MALONEY C, KALLIS MP, EDELMAN M, TZANAVARIS C, LESSER M et al.  
302 Gefitinib Inhibits Invasion and Metastasis of Osteosarcoma via Inhibition of Macrophage  
303 Receptor Interacting Serine-Threonine Kinase 2. *Mol Cancer Ther* 2020; 19: 1340-1350.  
304 <https://doi.org/10.1158/1535-7163.MCT-19-0903>
- 305 [10] XIE C, LIU S, WU B, ZHAO Y, CHEN B et al. miR-19 Promotes Cell Proliferation,  
306 Invasion, Migration, and EMT by Inhibiting SPRED2-mediated Autophagy in Osteosarcoma  
307 Cells. *Cell Transplant* 2020; 29: 963689720962460.  
308 <https://doi.org/10.1177/0963689720962460>
- 309 [11] ZHANG C, HUANG C, YANG P, LI C, LI M. Eldecalcitol induces apoptosis and  
310 autophagy in human osteosarcoma MG-63 cells by accumulating ROS to suppress the  
311 PI3K/Akt/mTOR signaling pathway. *Cell Signal* 2021; 78: 109841.  
312 <https://doi.org/10.1016/j.cellsig.2020.109841>
- 313 [12] VAN ALSTYNE M, LOTTI F, DAL MAS A, AREA-GOMEZ E, PELLIZZONI L.  
314 Stasimon/Tmem41b localizes to mitochondria-associated ER membranes and is essential for  
315 mouse embryonic development. *Biochem Biophys Res Commun* 2018; 506: 463-470.  
316 <https://doi.org/10.1016/j.bbrc.2018.10.073>
- 317 [13] MORETTI F, BERGMAN P, DODGSON S, MARCELLIN D, CLAERR I et al. TMEM41B  
318 is a novel regulator of autophagy and lipid mobilization. *EMBO Rep* 2018; 19: e45889.  
319 <https://doi.org/10.15252/embr.201845889>
- 320 [14] MORITA K, HAMA Y, IZUME T, TAMURA N, UENO T et al. TMEM41B Genome-wide  
321 CRISPR screen identifies as a gene required for autophagosome formation. *J Cell Biol* 2018;  
322 217: 3817-3828. <https://doi.org/10.1083/jcb.201804132>
- 323 [15] MORITA K, HAMA Y, MIZUSHIMA N. TMEM41B functions with VMP1 in  
324 autophagosome formation. *Autophagy* 2019; 15: 922-923.  
325 <https://doi.org/10.1080/15548627.2019.1582952>
- 326 [16] SHOEMAKER CJ, HUANG TQ, WEIR NR, POLYAKOV NJ, SCHULTZ SW et al.  
327 CRISPR screening using an expanded toolkit of autophagy reporters identifies Tmem41b as  
328 a novel autophagy factor. *PLoS Biol* 2019; 17: e2007044.  
329 <https://doi.org/10.1371/journal.pbio.2007044>
- 330 [17] WEI X, HE J, GAO B, HAN L, MAO Y et al. Hellebrigenin anti-pancreatic cancer effects  
331 based on apoptosis and autophagy. *PeerJ* 2020; 8: e9011. <https://doi.org/10.7717/peerj.9011>

- 332 [18] WANG Z, DENG Q, WANG Z, CHONG T. Effects of autophagy on the proliferation and  
333 apoptosis of clear cell renal carcinoma 786-O cells. *Int J Clin Exp Pathol* 2019; 12:  
334 1342-1349.
- 335 [19] LIU J, LIU Y, MENG L, JI B, YANG D et al. Synergistic Antitumor Effect of Sorafenib in  
336 Combination with ATM Inhibitor in Hepatocellular Carcinoma Cells. *Int J Med Sci* 2017;  
337 14: 523-529. <https://doi.org/10.7150/ijms.19033>
- 338 [20] WU JC, LAI CS, BADMAEV V, NAGABHUSHANAM K, HO CT et al.  
339 Tetrahydrocurcumin, a major metabolite of curcumin, induced autophagic cell death through  
340 coordinative modulation of PI3K/Akt-mTOR and MAPK signaling pathways in human  
341 leukemia HL-60 cells. *Mol Nutr Food Res* 2011; 55: 1646-1654.  
342 <https://doi.org/10.1002/mnfr.201100454>
- 343 [21] ASIEDU MK, THOMAS CF, DONG J, SCHULTE SC, KHADKA P et al. Pathways  
344 Impacted by Genomic Alterations in Pulmonary Carcinoid Tumors. *Clin Cancer Res* 2018;  
345 24: 1691-1704. <https://doi.org/10.1158/1078-0432.CCR-17-0252>
- 346 [22] KELLY AD, HAIBE-KAINS B, JANEWAY KA, HILL KE, HOWE E et al. MicroRNA  
347 paraffin-based studies in osteosarcoma reveal reproducible independent prognostic profiles  
348 at 14q32. *Genome Med* 2013; 5: 2. <https://doi.org/10.1186/gm406>
- 349 [23] ENNEKING WF, SPANIER SS, GOODMAN MA. A system for the surgical staging of  
350 musculoskeletal sarcoma. 1980. *Clin Orthop Relat Res* 2003; 415: 4-18.  
351 <https://doi.org/10.1097/01.blo.0000093891.12372.0f>
- 352 [24] ERGÜN S. Cross-Kingdom Gene regulation via miRNAs of *Hypericum perforatum* (St.  
353 John's wort) flower dietetically absorbed: An in silico approach to define potential  
354 biomarkers for prostate cancer. *Comput Biol Chem* 2019; 80: 16-22.  
355 <https://doi.org/10.1016/j.compbiolchem.2019.02.010>
- 356 [25] WEI J, MA Z, LI Y, ZHAO B, WANG D et al. MiR-143 inhibits cell proliferation by  
357 targeting autophagy-related 2B in non-small cell lung cancer H1299 cells. *Mol Med Rep*  
358 2015; 11: 571-576. <https://doi.org/10.3892/mmr.2014.267>
- 359 [26] MANCARELLA S, SERINO G, DITURI F, CIGLIANO A, RIBBACK S et al.  
360 Crenigacestat, a selective NOTCH1 inhibitor, reduces intrahepatic cholangiocarcinoma  
361 progression by blocking VEGFA/DLL4/MMP13 axis. *Cell Death Differ* 2020; 27:  
362 2330-2343. <https://doi.org/10.1038/s41418-020-0505-4>
- 363 [27] LIN YK, WU W, PONCE RK, KIM JW, OKIMOTO RA. Negative MAPK-ERK regulation  
364 sustains CIC-DUX4 oncoprotein expression in undifferentiated sarcoma. *Proc Natl Acad Sci*  
365 U S A 2020; 117: 20776-20784. <https://doi.org/10.1073/pnas.2009137117>
- 366 [28] MA K, ZHANG C, LI W. TGF- $\beta$  is associated with poor prognosis and promotes  
367 osteosarcoma progression via PI3K/Akt pathway activation. *Cell Cycle* 2020; 19:  
368 2327-2339. <https://doi.org/10.1080/15384101.2020.180555>
- 369 [29] NING L, WAN S, JIE Z, XIE Z, LI X et al. Lycorine Induces Apoptosis and G1 Phase  
370 Arrest Through ROS/p38 MAPK Signaling Pathway in Human Osteosarcoma Cells In Vitro  
371 and In Vivo. *Spine (Phila Pa 1976)* 2020; 45: E126-E139.  
372 <https://doi.org/10.1097/BRS.00000000000003217>
- 373

## 374 Figure Legends

375

376 **Figure 1.** Tmem41b is highly expressed in human osteosarcoma (OS) tissues. A) A subset of the  
377 differentially expressed mRNAs detected in the OS tissues (n=3) and control (n=3) using  
378 RNA-sequence. B) Ten mRNAs showing differential expression in the OS and normal aortic tissues  
379 were validated by the real-time quantitative polymerase chain reaction (RT-qPCR). Data represent  
380 mean±SD (n=3), \*p < 0.05 vs. control. C) Representative images of immunohistochemical staining  
381 for Tmem41b in OS tissues demonstrating negative, low, and high expressions. D) Overall survival  
382 curve of 103 osteosarcoma patients from the Second Hospital of Tangshan based on the Tmem41b  
383 mRNA level. E) The overall survival time in 262 osteosarcoma patients from the GEPIA (Gene  
384 Expression Profiling Interactive Analysis) dataset.

385  
386 **Figure 2.** Involvement of Tmem41b expression in the biological pathways of OS. A) Tmem41b  
387 expression levels in different OS cell lines (U87, U-2OS, and MG63) and human osteoblast cell line  
388 Hob (Normal) were evaluated by Western blot. The band intensities relative to β-actin are presented  
389 as mean±standard deviation (n=3; \*p < 0.05 vs. normal). B) QPCR verification of the knockdown  
390 efficiency of si-Tmem41b-transfected cells. Data represent mean±SD (n=3), \*\*\*p < 0.05 vs. si-NC.  
391 NC: negative control. n=3. C) U-2OS cells were transfected with si-NS or si-Tmem41b for 24 h,  
392 and total cell lysates were analyzed by Western blotting assay using the anti-Tmem41b, anti-LC3B  
393 and anti-p62 antibody. E) Enrichment plots from the gene set enrichment analysis (GSEA) of  
394 RNA-seq results in U-2OS cells were transfected with si-NC or si-Tmem41b. Several signaling  
395 pathways, including receptor activity, cell cycle, and metastasis was significantly decreased in  
396 si-Tmem41b group. F) U-2OS was transfected with si-NS or si-Tmem41b for 24 h and the levels of  
397 PCNA, Cyclin D1, Cyclin E1, and MMP13 were analyzed by Western blot. The band intensities  
398 relative to β-actin are presented as mean±standard deviation; n=3; \*p < 0.05 and \*\*p < 0.01 vs.  
399 si-NC

400  
401 **Figure 3.** Tmem41b down-regulation suppressed proliferation and migration of OS cells in vitro  
402 and in vivo. A) U-2OS cells were transfected with si-Tmem41b or si-NC RNA for 24 h, and a  
403 CCK8 assay was performed to determine the cell proliferation at different time points. \*p < 0.05  
404 and \*\*p < 0.01 vs. si-NC at corresponding time points. B) U-2OS cells were treated as described in  
405 (A), and a Transwell assay was conducted to detect the migration of the cells. Right: quantitative

406 analysis of cells that traversed the filter to the other side and were stained by hematoxylin and eosin.  
407 Data are expressed as mean±SEM from three independent experiments. \*\*p < 0.01 vs. si-NC. C)  
408 Knockdown of Tmem41b expression was measured by Western blotting. D) Tmem41b knockdown  
409 inhibited tumor growth in a nude mice xenograft model in vivo. E) Tumor volume and F) weight  
410 were measured after knockdown of Tmem41b expression. \*\*\*p < 0.001 compared with pLV-Vector  
411 group

412  
413 **Figure 4.** Down-regulation of Tmem41b suppressed MMP13 expression via AKT and p38 signaling  
414 pathways. A) Western blotting assay for signaling alteration of proliferation and invasion correlated  
415 with the p-AKT, p-ERK, and p-p38 pathway after Tmem41b knockdown in the U-2OS cells. Right:  
416 Band intensities were measured and normalized to β-actin and are shown below. \*p < 0.05 and \*\*\*p  
417 < 0.001, vs. total AKT, ERK, and p38 as well as β-actin (n=3). B) Representative images of  
418 immunohistochemical staining for Tmem41b in the OS tissues. Survival analysis showed that  
419 tumors with low Tmem41b expression have a favorable prognosis compared with those with high  
420 Tmem41b expression. C) The overall survival time of 150 osteosarcoma patients from the Second  
421 Hospital of Tangshan, based on the MMP13 protein level. D) The overall survival time of 259  
422 osteosarcoma patients, based on the MMP13 mRNA level from the GEPIA dataset.

423

424 **Table 1.** Association between Tmem41b expression and clinical characteristics in OS patients.

Parameter	Tmem41b expression (n=103)		p-value
	High (n=74)	Low (n=29)	
Age (years; mean±SEM)	23.8±6.2	25.4±7.7	0.323
Gender	Male	41	0.767
	Female	33	
Tumor size (cm)	5.96±0.48	6.25±0.29	0.004
Enneking's stage	□	9	0.737
	□A	27	
	□B	28	
	□	10	
Tumor location	Femur	32	0.813
	Fibula	14	
	Tibia	17	
	Humerus	5	
	Others	6	
Metastases	Lung	37	0.023
	Other	11	
Recurrence	No	26	0.036
	Yes	45	
	No	29	

425

Fig. 1 [Download full resolution image](#)

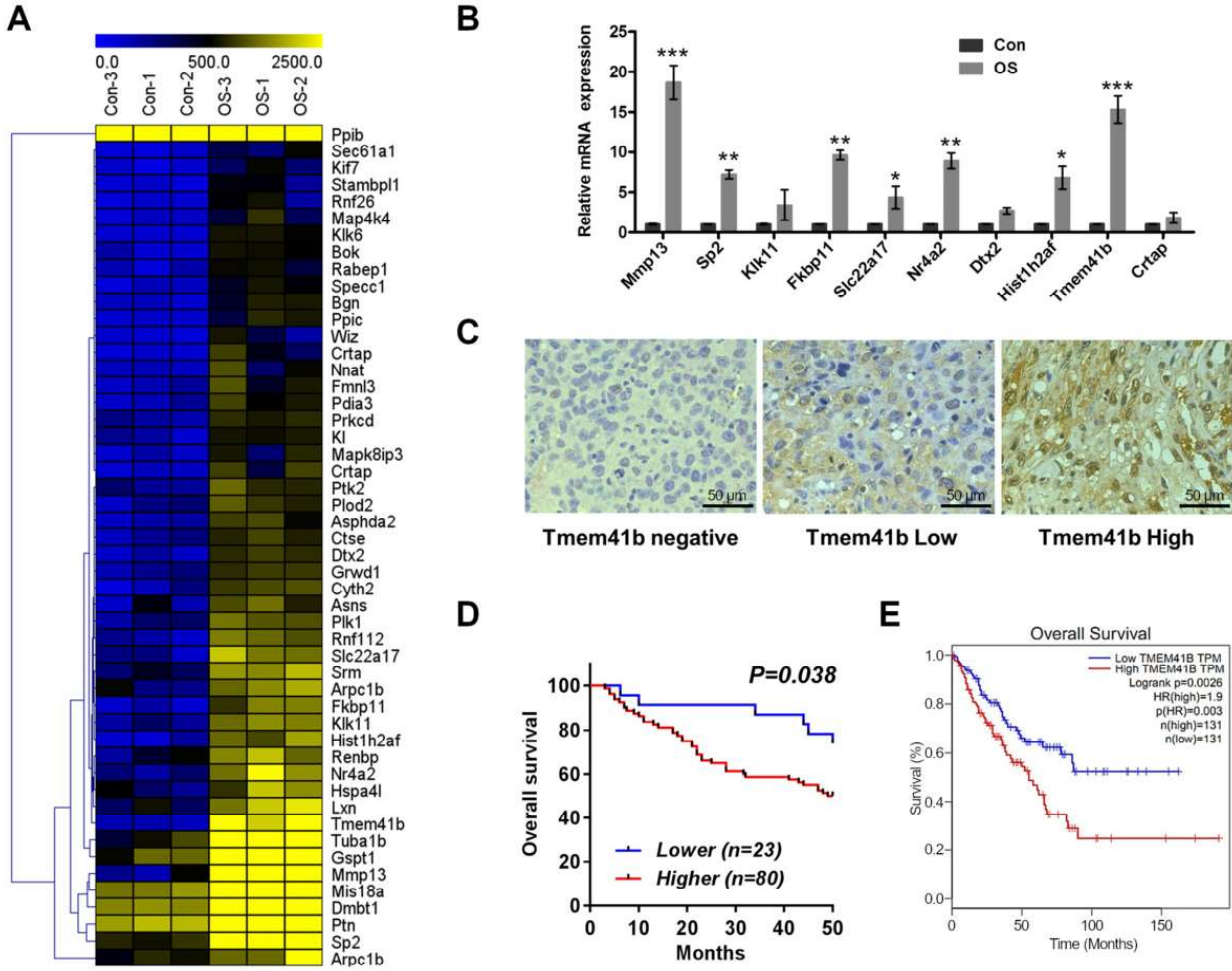


Fig. 2 [Download full resolution image](#)

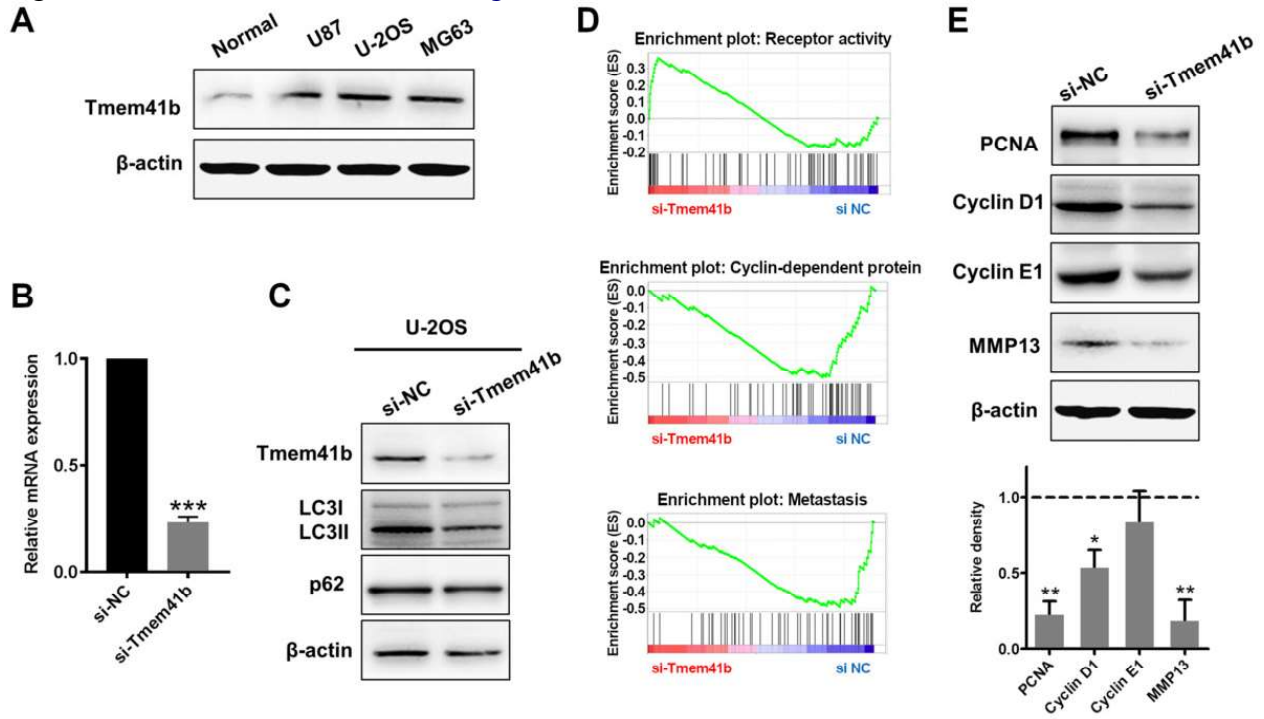


Fig. 3 [Download full resolution image](#)

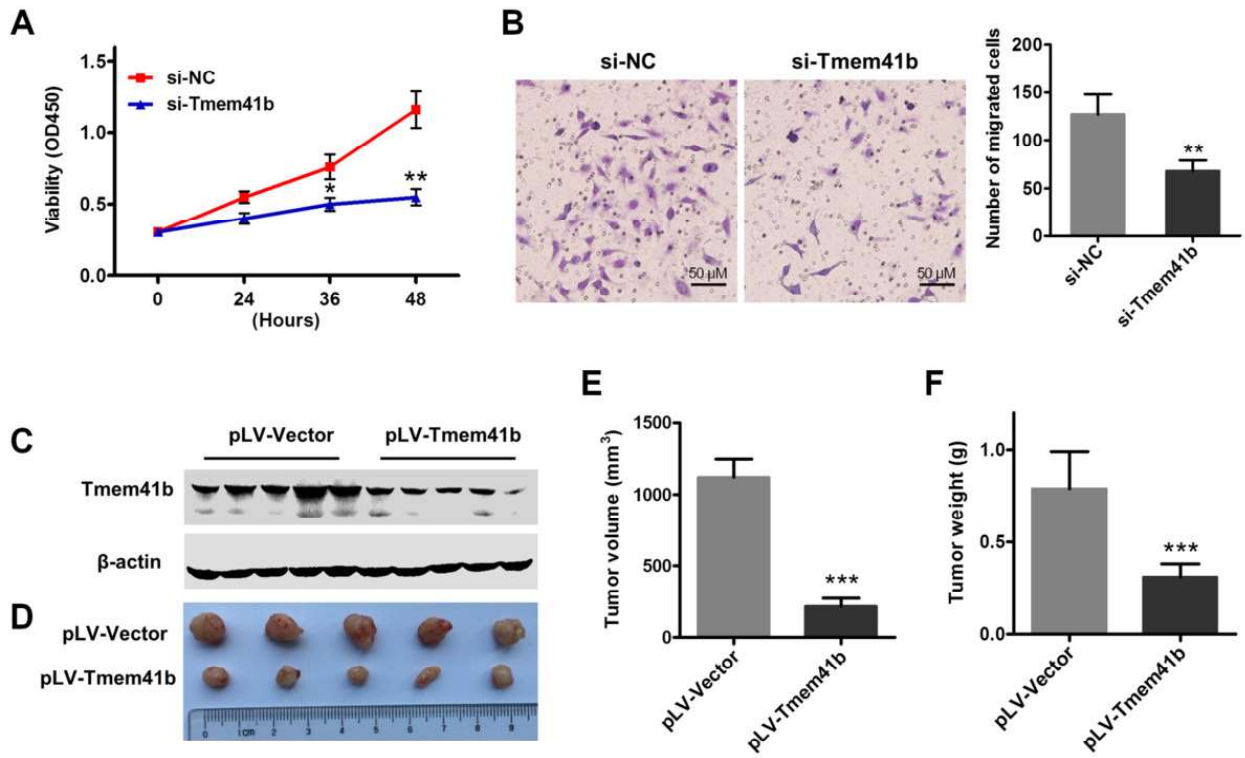
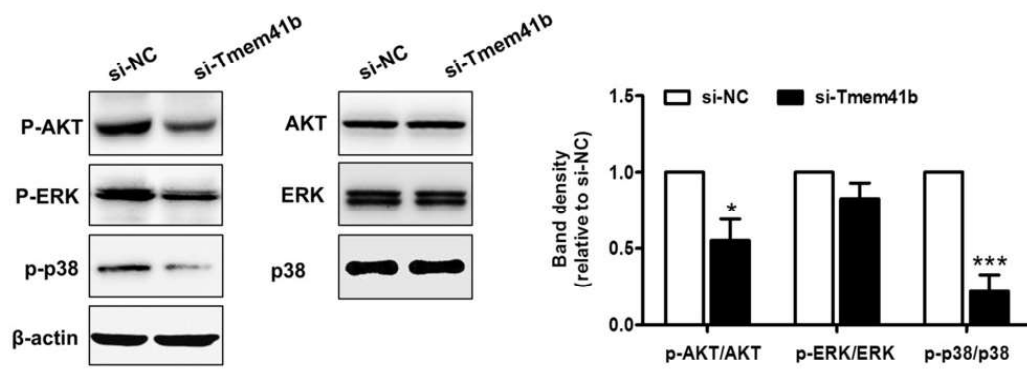
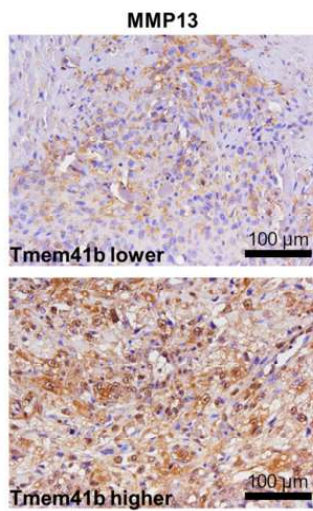


Fig. 4 [Download full resolution image](#)

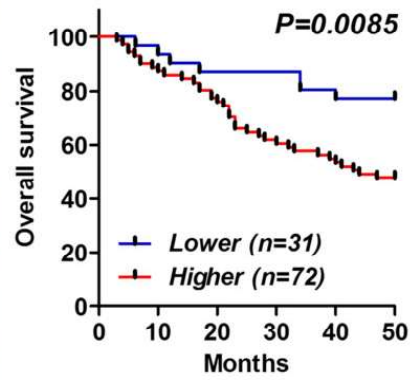
**A**



**B**



**C**



**D**

